

Bimodality and transient trimodality for Brownian particles in shear flows: A path-integral approach

Horacio S. Wio and Damián H. Zanette

Centro Atómico Bariloche and Instituto Balseiro, 8400 Bariloche, Río Negro, Argentina

(Received 29 June 1992)

The problem of Brownian motion in shear flows is analyzed using a path-integral approach and a piecewise-linearized velocity profile. In this way, the complete two-dimensional conditional probability distribution is found and the unimodal-bimodal transition in the longitudinal distribution is consistently described. A remarkable aspect is the appearance of a transient trimodal regime.

PACS number(s): 47.15.-x, 02.50.+s, 05.40.+j, 47.50.+d

Quite recently, the phenomenon of a Brownian particle moving in a medium with shear flow has been addressed in order to describe the faster-than-diffusive motion of tracer particles [1]. For the case of bidimensional systems, the model equation considered has the form

$$\partial_t P(x, y, t | x_0, y_0, t_0) = -V(y) \partial_x P + D \partial_{yy}^2 P, \quad (1)$$

where $P(x, y, t | x_0, y_0, t_0)$ is the conditional probability to reach the point (x, y) at time t , starting from (x_0, y_0) at t_0 ; $V(y)$ is the shear velocity field and D is the diffusion coefficient associated to the diffusive motion in the y direction. It is known that for a linear dependence of the velocity field on the coordinate y , the mean-square displacement grows in time as $\langle x(t)^2 \rangle \sim t^3$ [2,3]. For random velocity fields and within the continuous-time random-walk formalism, the exact asymptotic behavior of the first few nontrivial moments of the displacement has been found. This analysis has provided information about the scaling form for the marginal conditional probability $P(x, t) \propto \int dy P(x, y, t | x_0, y_0, t_0)$ [4]. The special case of power-law shear flows, $V(y) \propto \text{sgn}(y)y^\beta$, was recently considered. It was found that, varying the power β from $\beta=1$ to $\beta=0$, the marginal conditional probability $P(x, t)$ exhibits a transition from unimodal to bimodal behavior when a δ -function-like initial condition, $P(x_0, y_0, t_0) \propto \delta(x_0)\delta(y_0)$, is assumed [5]. By means of an effective velocity approximation, the critical value of β was estimated to be $\beta_c = 9/8$, at variance with a numerical result of $\beta_c \approx 0.75$.

In this paper, we present an alternative way to solve Eq. (1) through a path-integral approach [6,7]. It is well known that, when the associated Lagrangian is, at most, quadratic in coordinates and velocities, the path-integral representation for the conditional probability can be exactly integrated, for instance, by means of an expansion of the paths around a *reference* one ("classical," "macroscopic," or "most probable" path [7]). However, for the case of the power-law shear flow considered in Ref. [5], it is far from trivial to obtain the reference trajectory and, moreover, the above-mentioned path expansion does not stop at the second order in the coordinates. For this

reason, we have adopted an alternative form for the velocity field, according to

$$V(y) = v_0 \begin{cases} \epsilon y/a + (1 - \epsilon^2), & \epsilon a < y, \\ y/\epsilon a, & -\epsilon a < y < \epsilon a, \\ \epsilon y/a - (1 - \epsilon^2), & y < -\epsilon a, \end{cases} \quad (2)$$

where a and ϵ are constants ($0 \leq \epsilon \leq 1$). For $\epsilon=0$ and $\epsilon=1$, the form of the velocity field of Eq. (2) coincides with the power-law shear flow of Ref. [5] for the limit values $\beta=0$ and $\beta=1$, respectively. For intermediate values of ϵ and β , it is expected to be a convenient mimic of the power-law field. As a matter of fact, this linearization is the first step in a systematic polygonal approximation to the power-law velocity field, to be tested numerically in a forthcoming paper [8]. Such a piecewise-linearized version of the velocity field allows us to obtain the reference path and to perform the path integration by means of the path expansion procedure.

It is worth remarking that the Langevin equations equivalent to the Fokker-Planck equation (1), correspond to an uncorrelated additive white noise acting on the y variable [9]. The corresponding expression for the path-integral representation of the conditional probability is

$$P(x, y, t | x_0, y_0, t_0) = \int \mathcal{D}[x] \mathcal{D}[y] \mathcal{D}[p] \mathcal{D}[q] \exp\{-\mathcal{S}[x, y, p, q]\}, \quad (3)$$

where p and q are the conjugate "momentum" coordinates to x and y , respectively. The "action" $\mathcal{S}[x, y, p, q]$ is given by

$$\mathcal{S}[x, y, p, q] = \int_{t_0}^t ds \{ ip(s) [\dot{x}(s) - V(y(s))] + iq(s) \dot{y}(s) + Dq(s)^2 \}, \quad (4)$$

The Gaussian dependence on q allows us to integrate over this variable. The integral over p can also be done, leading to a δ -function-like functional, so that the functional integration over the x variable can be performed. We consider an initial condition given by $P(x_0, y_0, t_0) = \delta(x_0)\delta(y_0)$ with $t_0=0$; therefore, the notation can be

simplified by denoting $P(x, y, t) \equiv P(x, y, t | 0, 0, 0)$. Using a Fourier representation for the resulting delta function in x and $V(y)$, we obtain

$$P(x, y, t) = \int \frac{dk}{\sqrt{2\pi}} \exp[ik(x - x_0)] \mathcal{P}(y, t | y_0, 0), \quad (5)$$

$$\mathcal{P}(y, t) = \int \mathcal{D}[y] \exp \left[- \int_0^t ds \left[ikV(y(s)) + \frac{1}{4D} \dot{y}(s)^2 \right] \right].$$

The variation of the Lagrangian-like function in the exponent of the second path integral in Eqs. (5) yields the Euler-Lagrange equations for the most probable trajectory as

$$\ddot{y} - i2Dk\partial_y V(y) = 0, \quad (6)$$

to be solved with the boundary conditions $y(s=0)=0$ and $y(s=t)=y$. It is clear that the solutions to Eq. (6)

will correspond to complex trajectories. However, this fact introduces no major difficulties, as we can follow a similar approach as in Ref. [10], where this problem has been tackled and a WKB-like approach justified. In the present situation, the simplest way to perform the path integral in Eq. (5) is to use in Eq. (6) the boundary conditions in order to fix the real part of the trajectory, as the imaginary part becomes automatically determined by this result. The trajectory just found can be used as the reference path in the usual path expansion procedure [7].

Due to the symmetry of the problem, $P(x, y, t) = P(-x, -y, t)$, and it is sufficient to consider the positive values of y . As a consequence of the discontinuity in the potential $V(y)$, the reference trajectory discussed above is split according to the value of y being smaller or greater than ϵa . This implies that $P(x, y, t)$ is also split in two functional forms. For $y < \epsilon a$, we have

$$P(x, y, t) = (4\pi da^2 t)^{-1/2} \exp \left[- \frac{\eta^2}{4dt} \right] \left[\frac{12\epsilon^2}{dv_0^2 t^3} \right]^{1/2} \exp \left[- \frac{3\epsilon^2}{dv_0^2 t^3} (x - v_0 \eta t / 2\epsilon)^2 \right], \quad (7)$$

where $\eta = y/a$ is a scaled coordinate and $d = D/a^2$. For $y > \epsilon a$, the conditional probability is given by

$$P(x, y, t) = (4\pi da^2 t)^{-1/2} \exp \left[- \frac{\eta^2}{4dt} \right] \int \frac{dk}{\sqrt{2\pi}} \left[1 + 2i \frac{kv_0 dt^2}{\eta^2} \left[1 - \frac{\epsilon}{\eta} \right] (1 - \epsilon^2) \right]^{1/2} \\ \times \exp \left[- k^2 \frac{dv_0^2 t^3 \epsilon}{12\eta^2} \phi(\eta; \epsilon) + ik \psi(x, \eta; \epsilon) \right], \quad (8)$$

with

$$\phi(\eta; \epsilon) = \epsilon \eta^4 + 6\epsilon(1 - \epsilon^2)\eta^2 \\ + 4(1 - 2\epsilon^2)(1 - \epsilon^2)\eta - 3\epsilon(1 - \epsilon^2)^2, \quad (9)$$

$$\psi(x, \eta; \epsilon) = x - v_0 t \eta \left[\frac{\epsilon}{2} + (1 - \epsilon^2) \left[1 - \frac{\epsilon}{2\eta} \right] \eta \right].$$

For $\epsilon=1$ the above expression reduces to the one given by Eq. (7), as could be expected in complete agreement with the result in Ref. [3]. In this case, $P(x, y, t)$ is a multivariable Gaussian function, whose width increases as $t^{3/2}$ in the x direction and has normal diffusive behavior

$$P(x, y, t) \approx \frac{\eta^2}{v_0 dt^2} (4\pi da^2 t)^{-1/2} \exp \left[- \frac{\eta^2}{4dt} \right] \left[\frac{4dt}{\phi(\eta; \epsilon)} \right]^{1/2} \exp \left[- \left[\frac{\eta^2}{v_0 dt^2} \right]^2 \frac{dt}{\epsilon \phi(\eta; \epsilon)} \psi(x, \eta; \epsilon)^2 \right]. \quad (10)$$

In order to correct the jump arising at $y = \epsilon a$ due to the approximation above, we include in the last expression the factor $P(x, \epsilon a^-, t) / P(x, \epsilon a^+, t)$ and normalize the whole distribution to unity.

In Fig. 1, we show the conditional probability $P(x, y, t)$ for fixed values of ϵ and t , and $y > 0$. In part (a), the case

in the y direction.

According to a numerical analysis of the integrand in Eq. (8), it seems to be a reasonable approximation to neglect the second term in the prefactor square root. This is completely justified for small values of t . On the other hand, when t is large it would be more adequate to neglect the first term in the square root, leading to an exact solution in terms of the parabolic cylinder function $D_{1/2}(z)$. However, due to the compensation introduced by the slow damped oscillations of the integrand, the asymptotic behavior of this solution coincides with the result of neglecting the second term in the prefactor square root. A thorough discussion of the validity of such an approximation and its extensions will be given elsewhere [8]. Within this approximation, Eq. (8) reduces to

of a large value of ϵ is depicted and the quasi-Gaussian form of $P(x, y, t)$ is clearly seen. On the other hand, in part (b), for ϵ lower than a critical value ϵ_c to be defined later, we observe the appearance of a richer structure. We see that there is a hump located at the origin, as well as an additional hump, approximately situated at $x = v_0 t$.

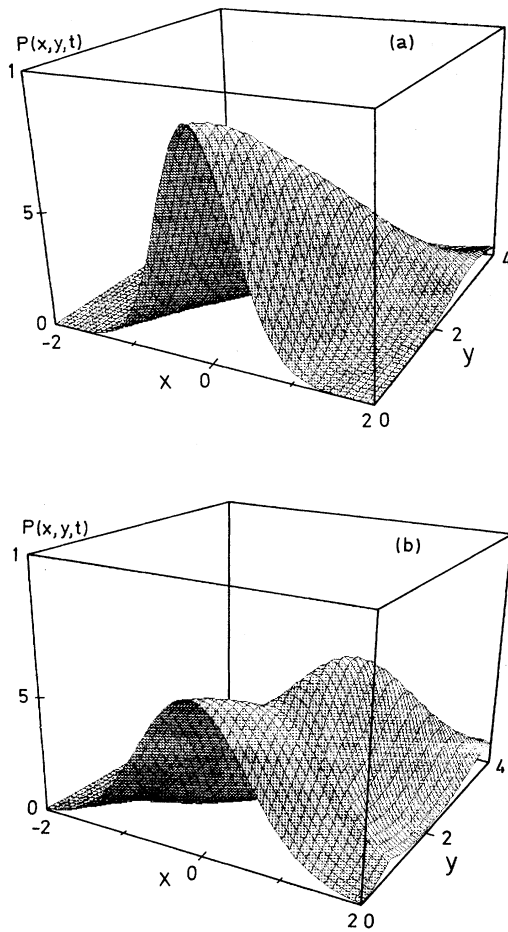


FIG. 1. The conditional probability $P(x,y,t)$ for fixed time, $t=1$, and positive values of y . (a) $\epsilon=0.9$; (b) $\epsilon=0.6$. Here and in the following figures, $a=1$, $d=1$, and $v_0=1$.

It is clear that there is a third hump symmetrically located with respect to the last one, i.e., in the lower plane and approximately centered at $x = -v_0 t$.

The trimodal behavior observed for $P(x,y,t)$ in the (x,y) plane explains the origin of bimodality in the marginalized conditional probability $P(x,t)$. In order to get this marginal probability, we must integrate $P(x,y,t)$ over y . For $-\epsilon a < y < \epsilon a$, the integration can be analytically done in terms of known functions, while we must resort to numerical procedures to evaluate the remaining contribution.

In Fig. 2, the marginal conditional probability $P(x,t)$ is depicted for fixed values of ϵ and several values of t . Part (a), corresponding to the results for a large value of ϵ , shows a unimodal behavior preserved as time elapses, in agreement with previous results [3,5]. Part (b), corresponding to results for $\epsilon < \epsilon_c$, makes it evident that a bimodal behavior appears at large times. This supports the arguments presented in Ref. [5], about the existence of a transition between the two regimes when changing the shear velocity profile. At variance with those results, the present approach allows us to obtain the complete conditional probability $P(x,y,t)$ as well as the marginal one,

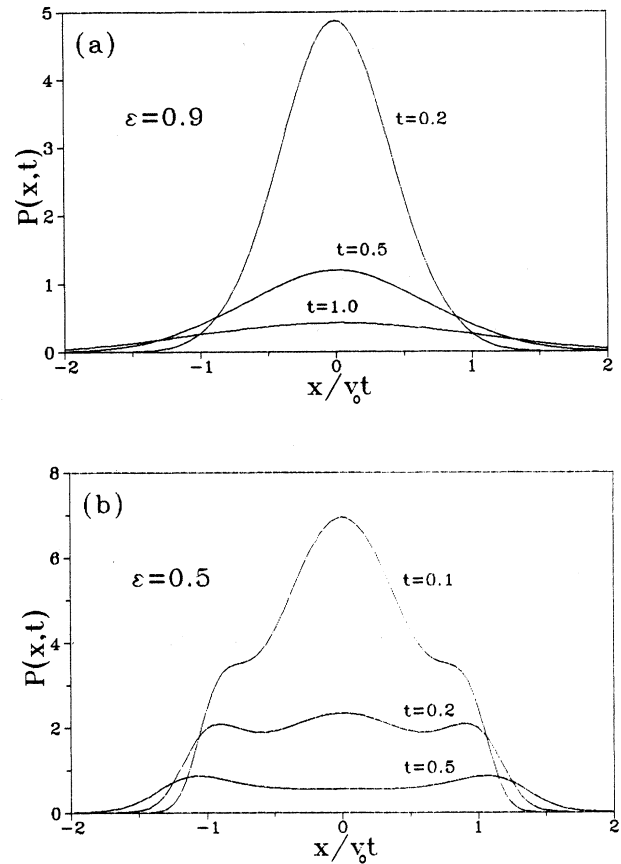


FIG. 2. The marginal conditional probability $P(x,t)$, as a function of the scaled variable $x/v_0 t$. (a) $\epsilon=0.9$ and $t=0.2, 0.5, 1.0$. For this value of ϵ , the behavior is clearly unimodal at every time. (b) $\epsilon=0.5$ and $t=0.1, 0.2, 0.5$. In this case, the transition from unimodal to bimodal behavior through a transient trimodal regime is apparent.

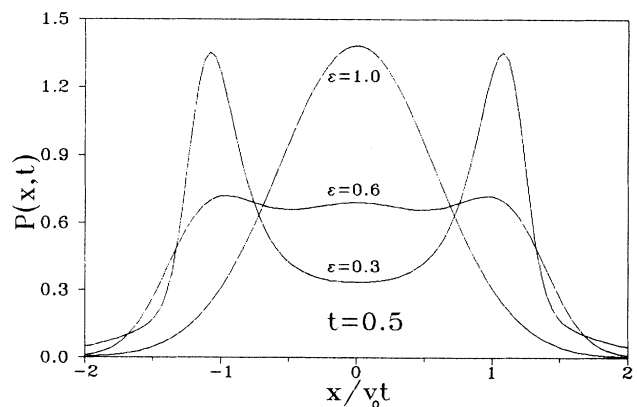


FIG. 3. The marginal conditional probability $P(x,t)$, as a function of the scaled variable $x/v_0 t$, for fixed time, $t=0.5$, and $\epsilon=1.0, 0.6, 0.3$. The transition from unimodal to bimodal behavior as a function of ϵ is clearly seen.

and to analyze their whole temporal evolution. As a by-product of this global result, we have also found that a transient *trimodality* in $P(x, t)$ occurs between the unimodal and the bimodal regimes. As a matter of fact, the fingerprints of trimodality are already seen in the unimodal distribution for short times.

In Fig. 3, $P(x, t)$ is plotted for a fixed time and various values of ϵ . Varying ϵ from large to small values, the transition between unimodal, trimodal, and bimodal behaviors is apparent.

As seen in Fig. 3, the critical point ϵ_c for the occurrence of the transition between the unimodal and the bimodal regime is not clearly defined. This is due to the existence of the intermediate trimodal regime which diffuses the transition. Indeed, in the critical region, the maximum of the unimodal distribution becomes more and more flat before the appearance of the three humps. As a criterion for the determination of ϵ_c , we have chosen the limit value for which no trimodal behavior arises as time elapses, giving $\epsilon_c \approx 0.87$. In order to relate our parameter ϵ to the exponent β in the power-law shear velocity profile [5], we required that the deterministic behavior of a particle initially situated at the origin should yield the same time to reach the point $y=1$ in both

descriptions. This gives a good agreement with the critical value obtained for β_c by numerical means in Ref. [6].

A main aspect of our results is the appearance of the intermediate trimodal regime, taking place between the unimodal and the bimodal one, when $\epsilon < \epsilon_c$. An extensive numerical analysis of $P(x, t)$ suggests that this transient state occurs systematically and is not restricted to particular values of the parameters. This fact seems to be of a more general character, in the sense that such transient trimodal behavior also appears in other bistabilitylike problems [11].

A deeper analysis of the approximations completed to obtain Eq. (10), as well as the way to overcome them, is underway. A better comparison between this piecewise-linearized velocity profile and the power-law one, based on numerical simulations of this convection-diffusion problem, will also be the subject of further work [8].

The authors thank Professor D. ben-Avraham for fruitful discussions and for calling their attention to this problem, and Dr. V. Grunfeld for a careful reading of the manuscript. Financial support from CONICET (PIA 0523/91) and Fundación Antorchas, Argentina, is gratefully acknowledged.

-
- [1] D. ben-Avraham, F. Leyvraz, and S. Redner, *Phys. Rev. A* **45**, 2315 (1992).
 - [2] G. K. Batchelor, *J. Fluid Mech.* **95**, 369 (1979); R. T. Foister and T. G. M. Van De Ven, *ibid.* **96**, 105 (1980).
 - [3] R. Mauri and S. Haber, *SIAM J. Appl. Math.* **46**, 49 (1986).
 - [4] G. Zumofen, J. Klafter, and A. Blumen, *Phys. Rev. A* **42**, 4601 (1990).
 - [5] E. Ben-Naim, S. Redner, and D. ben-Avraham, *Phys. Rev. A* **45**, 7207 (1992).
 - [6] R. P. Feynmann and A. R. Hibbs, *Quantum Mechanics and Path Integrals* (McGraw-Hill, New York, 1965).
 - [7] F. Langouche, D. Roekaerts, and E. Tirapegui, *Functional*

Integration and Semiclassical Expansions (Reidel, Dordrecht, 1982).

- [8] G. Marshall, H. S. Wio, and D. H. Zanette (unpublished).
- [9] N. G. Van Kampen, *Stochastic Processes in Physics and Chemistry* (North-Holland, Amsterdam, 1981); C. W. Gardiner, *Handbook of Stochastic Methods* (Springer, Berlin, 1983).
- [10] J. C. Garrison and E. M. Wright, *Phys. Lett.* **108A**, 129 (1985).
- [11] G. Abramson, H. S. Wio, and L. D. Salem, in *Nonlinear Phenomena in Fluids, Solids and Other Complex Systems*, edited by P. Cordero and B. Nachtergaele (Elsevier, New York, 1991), p. 373.